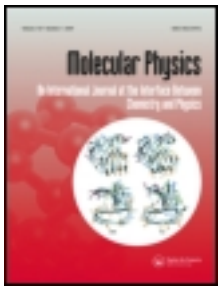

Molecular Physics: An International Journal at the Interface Between Chemistry and Physics
Publication details, including instructions for authors and subscription information:
http://www.tandfonline.com/loi/tmph20

A geometric approach to direct minimization

TROY VAN VOORHIS [a] & MARTIN HEAD-GORDON [a]
[a] Department of Chemistry, University of California, Berkeley, CA, 94720, USA

Version of record first published: 01 Dec 2009.

To cite this article: TROY VAN VOORHIS & MARTIN HEAD-GORDON (2002): A geometric approach to direct minimization, Molecular Physics: An International Journal at the Interface Between Chemistry and Physics, 100:11, 1713-1721

To link to this article: http://dx.doi.org/10.1080/00268970110103642

MOLECULAR PHYSICS, 2002, VOL. 100, NO. 11, 1713–1721

Taylor & Francis
Taylor & Francis Group

A geometric approach to direct minimization

TROY VAN VOORHIS and MARTIN HEAD-GORDON*
Department of Chemistry, University of California, Berkeley, CA 94720, USA

(*Received 2 June 2001; accepted 9 October 2001*)

The approach presented, geometric direct minimization (GDM), is derived from purely geometrical arguments, and is designed to minimize a function of a set of orthonormal orbitals. The optimization steps consist of sequential unitary transformations of the orbitals, and convergence is accelerated using the Broyden–Fletcher–Goldfarb–Shanno (BFGS) approach in the iterative subspace, together with a diagonal approximation to the Hessian for the remaining degrees of freedom. The approach is tested by implementing the solution of the self-consistent field (SCF) equations and comparing results with the standard direct inversion in the iterative subspace (DIIS) method. It is found that GDM is very robust and converges in every system studied, including several cases in which DIIS fails to find a solution. For main group compounds, GDM convergence is nearly as rapid as DIIS, whereas for transition metal-containing systems we find that GDM is significantly slower than DIIS. A hybrid procedure where DIIS is used for the first several iterations and GDM is used thereafter is found to provide a robust solution for transition metal-containing systems.

1. Introduction

The optimization of one-particle orbitals in quantum chemistry is a significant undertaking because, although often one can readily derive a set of equations that the optimal orbitals must satisfy, usually it is not so simple to obtain a rapid solution to these equations. The DIIS method [1, 2] has proved an extremely effective solution to this problem for both SCF and correlated wavefunctions [3–7]. With DIIS, one determines the linear combination of previous gradients that has minimum length and then uses this information to extrapolate a new step that should have a small gradient, and therefore be nearly stationary. DIIS is certainly the most used convergence algorithm in quantum chemistry today, and often it is extraordinary how well it works. However, it is not without weaknesses. The central difficulty is that in the case of near-degeneracies or other pathologies one sometimes finds that the DIIS iterations simply fail to converge to any solution, which clearly is frustrating for the user. This deficiency stems from the fact that DIIS is an extrapolation procedure rather than a minimization algorithm; even a simple conjugate gradient approach is guaranteed eventually to converge to a minimum. Unfortunately, what one really desires is a method that is both robust and rapidly convergent, and conjugate gradient alone requires far too many iterations in practice. Other gradient-based direct minimization algorithms have been proposed [8–10] but have not proved nearly as useful as the DIIS ansatz. Direct minimization algorithms exploiting Hessian-like matrices [11–13] generally converge much faster than even DIIS, but in most cases inverting the Hessian to obtain the Newton–Raphson step is computationally expensive. In this work, we present a direct minimization algorithm that requires only gradient information, converges at essentially the same rate as DIIS for 'easy' cases, and is capable of converging cases where DIIS fails.

* Author for correspondence. e-mail: mhg@cchem.berkeley.edu

2. Theory

Our treatment is based on the geometric approach to orthogonality constraints presented by Edelman *et al.* [14]. Their formalism is very general, and we review only the crucial results here; the interested reader is directed to the original article for more information. For clarity, we shall specialize to the case of SCF orbital optimization, but it should be clear that generalizations to other methods that require orbital optimization can be made readily.

2.1. *The SCF equations*

Begin with a set of N orthonormal orbitals $\{\phi_i\}$ that are written as a linear combination of a set of N (not necessarily orthogonal) basis functions $\{\chi_\mu\}$,

$$\phi_i(r) = \sum_{\mu=1}^{N} \chi_\mu(r) C_{\mu i}. \tag{1}$$

In SCF theory, the objects of fundamental interest are the orthonormal orbitals

Molecular Physics ISSN 0026–8976 print/ISSN 1362–3028 online © 2002 Taylor & Francis Ltd
http://www.tandf.co.uk/journals
DOI: 10.1080/00268970110103642

$$\psi_i(r) = \sum_{\mu=1}^{N} \chi_\mu(r) D_{\mu i} \tag{2}$$

that minimize an (as yet unspecified) energy functional. This energy actually only depends on the first M of these orthogonal functions; the remaining orbitals contain no electrons and therefore have no effect on the energy. The presence of $N - M$ additional 'virtual' orbitals is convenient, since it turns what would be a rectangular coefficient matrix $\mathbf{C}$ into a square matrix.

Since the sets $\{\phi_i\}$ and $\{\psi_i\}$ are both orthonormal, we can write the optimal set of coefficients as a unitary transformation of the initial set:

$$\mathbf{D} = \mathbf{CU}, \tag{3}$$

where $\mathbf{U}$ is a unitary matrix. Thus, we seek to minimize the energy $E(\mathbf{U}, \alpha)$ as a function of the unitary matrix $\mathbf{U}$, holding fixed any other degrees of freedom, α, that the energy may depend upon (e.g. nuclear degrees of freedom, coupled-cluster amplitudes). One can obtain Hartree–Fock or Kohn–Sham theory from this energy, depending on how $E(\mathbf{U}, \alpha)$ is defined. Since none of what follows depends on the distinction between these forms for the energy, we shall leave the definition of $E(\mathbf{U}, \alpha)$ intentionally vague so that our SCF algorithm will apply without modification to both Hartree–Fock and Kohn–Sham approaches. We can enforce the unitarity constraint

$$\mathbf{U}^\dagger \mathbf{U} = \mathbf{1}, \tag{4}$$

where $\mathbf{1}$ represents the unit matrix, by defining a matrix of Lagrange multipliers ϵ and finding the stationary points of the associated functional

$$\tilde{E}(\mathbf{U}, \alpha) = E(\mathbf{U}, \alpha) - \mathrm{Tr}[\epsilon \cdot (\mathbf{U}^\dagger \mathbf{U} - \mathbf{1})]. \tag{5}$$

The stationary equations give the unitarity condition on $\mathbf{U}$, (equation (4)), and

$$\frac{\partial E}{\partial \mathbf{U}} \equiv \mathbf{F}(\mathbf{U}) = \epsilon \cdot \mathbf{U}^\dagger \tag{6}$$

where we have defined the Fock matrix, $\mathbf{F}$, which is in general a nonlinear function of U. Equation (6) is the familiar Roothaan equation [15] that leads to an iterative procedure where one diagonalizes $\mathbf{F}$ to obtain a new estimate for $\mathbf{U}$, which is then used to build a new $\mathbf{F}$, which may be diagonalized ... This is one particular formulation of the SCF optimization problem we wish to solve.

We note here that for both DFT and HF the energy does not depend on the M occupied orbitals individually, but only on the space that they span. A manifold with this type of invariance is called a Grassmann manifold, and many of the results we shall present depend upon the existence of such an invariant subspace. This excludes certain generalized valence bond [16] and optimized effective potential methods [17] but includes most coupled-cluster approaches [7, 18] and many active-space correlation models [6, 19]. Finally, often in what follows it is useful to exploit the distinction between 'occupied' and 'virtual' subspaces and depict matrices in terms of their occupied–occupied (oo), virtual–virtual (vv) occupied–virtual (ov) and virtual–occupied (vo) blocks. For example,

$$\mathbf{U} \equiv \begin{pmatrix} \mathbf{U}_{oo} & \mathbf{U}_{ov} \\ \mathbf{U}_{vo} & \mathbf{U}_{vv} \end{pmatrix}. \tag{7}$$

2.2. *A geometric approach*

If we consider the space of all unitary matrices as a manifold embedded in the larger space of all matrices, we see that the constraint (4) forces the manifold to be curved. This can be illustrated readily by considering the analogous problem in 3 dimensions of minimizing a function subject to the constraint

$$\mathbf{x} \cdot \mathbf{x} = 1. \tag{8}$$

Of course, the manifold of possible solutions in this case is the unit sphere, which is a curved surface.

If we make an infinitesimal change $\mathbf{U} \rightarrow \mathbf{U} + \delta\mathbf{U}$ and apply the unitarity constraint (4) to the new matrix, we find that the variation $\delta\mathbf{U}$ must satisfy the equation

$$\mathbf{U}^\dagger \delta\mathbf{U} + \delta\mathbf{U}^\dagger \mathbf{U} = \mathbf{0} \tag{9}$$

where terms second order in the infinitesimal have been neglected. Notice that this constraint is linear in $\delta\mathbf{U}$; thus the subspace of allowable infinitesimal variations is a linear space (the tangent space) that has no curvature. To first order, movement in this space is identical to movement on our curved manifold. Thus, the tangent space is the flat space that is locally most like our curved manifold, and it plays a central role in the translation of any algorithm designed to work on a flat manifold into one that works in a curved space.

Since the SCF energy is invariant to transformations of the occupied and virtual subspaces amongst themselves, changes in the energy must therefore be due to ov and vo transformations alone. In this context, we can divide the space of tangent vectors into 'horizontal' vectors ($\mathbf{H}$) that do not affect the energy and 'vertical' vectors ($\mathbf{V}$) that can change the energy (here our convention for 'vertical' and 'horizontal' vectors is opposite to the standard convention),

$$\mathbf{H} \equiv \begin{pmatrix} \mathbf{H}_{oo} & \mathbf{0} \\ \mathbf{0} & \mathbf{H}_{vv} \end{pmatrix}, \qquad \mathbf{V} \equiv \begin{pmatrix} \mathbf{0} & \mathbf{V}_{ov} \\ \mathbf{V}_{vo} & \mathbf{0} \end{pmatrix}. \tag{10}$$

Clearly, in order to optimize the SCF orbitals we need deal only with the vertical space. In the special case $\mathbf{U} = \mathbf{1}$, the tangent space condition (9) implies that

variations in **U** must be skew-symmetric. Thus, in this important case, the vertical vectors are defined by their ov block alone,

$$\mathbf{V} = \begin{pmatrix} \mathbf{0} & \mathbf{V}_{ov} \\ -\mathbf{V}_{ov}^{\dagger} & \mathbf{0} \end{pmatrix}. \tag{11}$$

The vertical tangent vectors allow us to create geodesics. A geodesic is the shortest path in our curved manifold that connects two given points [20]. It is also the 'straightest' curve available on the surface, since additional curvature would tend to lengthen the path. Hence, on a curved surface, one discards the notion of a straight line and replaces it with that of a geodesic. For SCF the geodesics depend only on the vertical vectors; horizontal moves do not affect the energy, and thus any transformation in the horizontal space will tend to unnecessarily lengthen the path to the minimum. Given a vertical vector **V**, it may be shown [14] that the geodesic initially tangent to **V** may be written explicitly as

$$\mathbf{U}(\mathbf{V}) = e^{\mathbf{V}}. \tag{12}$$

Therefore, a given vertical tangent vector **V** defines the initial direction of a unique geodesic.

If we define $\mathbf{X} = \mathbf{V}_{ov}\mathbf{V}_{vo}$ and $\mathbf{Y} = \mathbf{V}_{vo}\mathbf{V}_{ov}$ it is easily verified that [21]

$$\mathbf{U}(\mathbf{V}) = \begin{pmatrix} \cos \mathbf{X}^{1/2} & \mathbf{X}^{-1/2} \sin \mathbf{X}^{1/2}\mathbf{V}_{ov} \\ \mathbf{V}_{vo}\mathbf{X}^{-1/2} \sin \mathbf{X}^{1/2} & \cos \mathbf{Y}^{1/2} \end{pmatrix}. \tag{13}$$

This allows the geodesic to be evaluated in $O(N^3)$ time, with the key step being the diagonalizations of **X** and **Y**. We can now formulate steepest descent on the Grassmann manifold:

(1) Obtain an initial set of (orthogonal) orbital coefficients $\mathbf{C}_0$.

(2) Compute the gradient,

$$\mathbf{G} = \frac{dE}{d\mathbf{V}} = \frac{dE}{d\mathbf{U}}\frac{d\mathbf{U}}{d\mathbf{V}} = \mathbf{F}\frac{d\mathbf{U}}{d\mathbf{V}}$$

evaluated with the current set of orbitals. This is a vertical vector in the tangent space.

(3) Minimize the energy along the geodesic defined by **G**. That is, minimize

$$E(\gamma) = E(e^{\gamma \mathbf{G}}, \alpha) \tag{14}$$

as a function of γ. Let γ_0 denote the optimal value of γ.

(4) Update the orbitals using

$$\mathbf{C}_{i+1} = \mathbf{C}_i e^{\gamma_0 \mathbf{G}}. \tag{15}$$

(5) If convergence has not been achieved, return to step 2.

Note that this requires one to perform a sequence of unitary transformations rather than attempting to write the final set of orbital coefficients as a single unitary transformation of the initial set. That is, the final set of orbitals is written

$$\mathbf{C} = \mathbf{C}_0 e^{\Delta_0} e^{\Delta_1} e^{\Delta_2} \ldots e^{\Delta_n}, \tag{16}$$

where each Δ_i is a scaled gradient rather than

$$\mathbf{C} = \mathbf{C}_0 e^{\Delta}, \tag{17},$$

and where Δ must be determined. Clearly the former approach can be viewed as a special case of the latter where the orbitals are 're-set' at each iteration. This amounts to shifting the origin of our reference frame to the current set of orbitals as opposed to referencing it to the arbitrary initial orbitals.

2.3. *Approximate Hessian approach*

The use of the gradient as the step direction, as in steepest descent, is far from optimal in practice; to improve upon this step, one must utilize second-derivative information. Approximate Hessian methods accomplish this by employing the Newton–Raphson-like step

$$\mathbf{S} = -\mathbf{B}\mathbf{G}, \tag{18}$$

where **G** is the gradient and **B** is an approximation to the inverse Hessian constructed from vectors collected in previous iterations. In a curved manifold, one needs to be sure that the previous vectors are contained in the current tangent space before constructing the approximate Hessian; otherwise the resulting step direction might not be tangent to our surface, making it impossible to construct the relevant geodesic. It is at this point that the formulation of 're-setting' the orbitals at each iteration becomes useful. Specifically, since re-setting the orbitals amounts to setting $\mathbf{U} = \mathbf{1}$ at the beginning of each iteration, we have at every iteration that the tangent space is of the form of equation (11), and therefore the tangent vectors from previous iterations are guaranteed to be in the tangent space at the current point. If we had chosen a fixed frame, the tangent spaces could not possibly be the same because this would imply that our surface was flat.

Now, the fact that the tangent spaces of subsequent iterations are the same does not necessarily imply that individual vectors in these spaces may be identified; there could be some significant internal shuffling of tangent vectors between iterations that does not affect the space they span. Rigorously, one should obtain vectors in the current frame by transporting the previous vectors along the relevant geodesic, making sure to keep the angle between each vector and the geodesic fixed. Such a process is called parallel transport, and we may denote the vertical vector **V** after parallel transport by $\tau\mathbf{V}$. For

a Grassmann manifold, Edelman *et al.* [14] showed that the parallel transport of $\mathbf{V}$ along the geodesic generated by Δ is given by

$$\tau\mathbf{V} = e^{\Delta}\mathbf{V}. \tag{19}$$

However, the unitary transformation e^{Δ} is absorbed into the definition of $\mathbf{C}$ when we re-set our orbitals and therefore the parallel transported vector $\tau\mathbf{V}$ in the rotated frame is identical to the original vector $\mathbf{V}$. We stress that this is a special feature of the Grassmann manifold in particular, and methods with invariant subspaces in general. In situations with no invariant subspaces, such simplifications do not occur and parallel transport must be explicitly accounted for explicitly. However, for the Grassmann case, setting $\mathbf{U} = \mathbf{1}$ every iteration successfully rotates the frame of reference so that the new tangent space in the new frame is identical to the old tangent space in the old frame, and parallel transport is unnecessary.

One may now apply the BFGS update scheme [22] in which the approximate inverse Hessian for the $(i+1)$th iteration can be written as

$$\mathbf{B}_{i+1}(\mathbf{S}_i, \delta\mathbf{G}_{i+1}, \mathbf{B}_i) = \mathbf{B}_i + \frac{\mathbf{S}_i \otimes \mathbf{S}_i}{\mathbf{S}_i \cdot \delta\mathbf{G}_{i+1}} + \mathrm{GBG}\,\mathbf{u} \otimes \mathbf{u} - \frac{(\mathbf{B}_i \cdot \delta\mathbf{G}_{i+1}) \otimes (\mathbf{B}_i \cdot \delta\mathbf{G}_{i+1})}{\mathrm{GBG}}, \tag{20}$$

where $\delta\mathbf{G}_{i+1}$ is the change in the gradient vector from the previous iteration and the intermediates

$$\mathbf{u} = \frac{\mathbf{S}_i}{\mathbf{S}_i \cdot \delta\mathbf{G}_{i+1}} - \frac{\mathbf{B}_i \cdot \delta\mathbf{G}_{i+1}}{\mathrm{GBG}}$$

and

$$\mathrm{GBG} = \delta\mathbf{G}_{i+1} \cdot \mathbf{B}_i \cdot \delta\mathbf{G}_{i+1} \tag{21}$$

have been used. The BFGS Hessian has two nice properties that make it well suited to minimization problems. First, it minimizes a quadratic potential with the minimum number of gradient evaluations, and therefore is expected to have superlinear convergence. Second, the BFGS Hessian is positive definite. Hence, given the choice between reducing the energy in one direction and reducing the gradient in another, the BFGS prescription will tend to preferentially reduce the energy, which clearly is desirable when dealing with a minimization problem.

Storing the BFGS Hessian is not difficult, because one needs only to compute it in the subspace spanned by gradients and steps from previous iterations. This is easily accomplished by orthonormalizing the vectors from previous iterations and expanding everything in terms of these orthogonal basis vectors [8]. Since the size of the subspace is not expected to depend strongly on the size of the system, the construction and storage of the approximate Hessian is never prohibitive.

Unfortunately, BFGS by itself does not accelerate convergence enough to be competitive with DIIS. This is because the orbital rotation space has many dimensions and therefore BFGS requires many iterations in order to build up enough information about the Hessian. It would be ideal if we could incorporate an approximate Hessian for the degrees of freedom not spanned by previous iterations and simply update this Hessian using BFGS as more and more degrees of freedom are explored. One way to do this is to diagonalize the oo and vv blocks of the Fock matrix. The approximate Hessian can then be chosen to be diagonal and equal to the difference in orbital eigenvalues $\{\epsilon\}$ at the current iteration [8, 9, 23]:

$$B_{ia,jb} = 2(\epsilon_a - \epsilon_i)\delta_{ij}\delta_{ab} \tag{22}$$

where i, j and a, b represent occupied and virtual orbital indices, respectively. However, following the work of Bacskay [11, 12], we note that the optimal diagonal Hessian actually contains an energy shift,

$$B_{ia,jb} = 2(\epsilon_a - \epsilon_i + \delta E)\delta_{ij}\delta_{ab}. \tag{23}$$

Within Bacskay's quadratic procedure, the value of this shift is equal to the change in energy that results from a Newton–Raphson step using the shifted Hessian. Since clearly the energy that would be obtained after application of the Hessian clearly cannot be determined before the Hessian has been constructed, it must be estimated in practice. We find that the energy change from the previous iteration is a reasonable estimator, and this choice actually greatly improves the rate and stability of convergence in the early iterations. In order to interface this approximate Hessian with the BFGS scheme, we note that before any iterations have occurred the BFGS Hessian is the unit matrix. Following [8], we can transform to the set of coordinates where our diagonal Hessian (23) is also the unit matrix

$$G_{ia} \rightarrow \frac{G_{ia}}{B_{ia,ia}^{1/2}}, \tag{24}$$

which we will call the energy-weighted coordinates (EWCs). The BFGS prescription (20) can then be applied in terms of these coordinates.

To compute the EWCs (equation (24)) one must find the orbitals that diagonalize the oo and vv blocks of the Fock matrix: the pseudo-canonical orbitals. Since this does not affect the energy, the relevant transformation can be written as a step in the horizontal space,

$$\tilde{\mathbf{C}} = \mathbf{C}e^{\mathbf{H}}; \qquad \mathbf{H} = \begin{pmatrix} \mathbf{H}_{oo} & \mathbf{0} \\ \mathbf{0} & \mathbf{H}_{vv} \end{pmatrix}. \tag{25}$$

It is easy to verify that taking a gradient step before making the pseudo-canonical transform is not equivalent to performing the same operations in the opposite order,

$$\tilde{\mathbf{C}} = \mathbf{C}e^{\mathbf{G}}e^{\mathbf{H}} \neq \mathbf{C}e^{\mathbf{H}}e^{\mathbf{G}}, \tag{26}$$

and therefore we must be very careful about the order of these two steps. In order to convert to the current set of EWCs, we must pseudo-canonicalize first and then compute the gradient; however, for vectors from previous iterations clearly this is not possible. Thus, in order to treat the previous steps and gradients on an equal footing with the current gradient, we must determine how the pseudo-canonical rotation affects vertical tangent vectors from previous iterations. Specifically, we desire the vector $\tilde{\mathbf{V}}$ that satisfies

$$e^{\mathbf{H}}e^{\tilde{\mathbf{V}}} = e^{\mathbf{V}}e^{\mathbf{H}} \tag{27}$$

for an arbitrary vertical vector $\mathbf{V}$ (e.g. the gradient). Clearly $\tilde{\mathbf{V}}$ is the analogue of $\mathbf{V}$ in the current frame. It is readily verified that the correct solution is

$$\tilde{\mathbf{V}} = e^{\mathbf{H}^{\dagger}}\mathbf{V}e^{\mathbf{H}}. \tag{28}$$

This is just a consequence of the standard transformation rules for a matrix under a unitary transformation of the coordinates. Therefore, it is possible to update the EWCs at every iteration so long as one transforms the gradients and steps from previous iterations using equations (28). Clearly, changing the EWCs at every iteration is beneficial, as it allows one always to use the 'best' approximate Hessian at the current point. Previous algorithms [8, 9, 23] have been forced to retain the EWCs from the initial set of orbitals. This is fine as long as the orbitals do not change very much, but is a serious limitation in general, because the quality of the diagonal Hessian (23) will degrade as one moves away from the reference point.

There is a simple geometric interpretation of this transformation in terms of trajectories on our curved manifold, as depicted in cartoon form in figure 1. During the first iteration, we begin with an initial set of orbitals $\mathbf{C}_0$ and follow a vertical step $\mathbf{V}$ to obtain a new set of orbitals, $\mathbf{C}_1$. We then pseudo-canonicalize the orbitals by following a horizontal vector $\mathbf{H}$. As is clear in the figure, there is no vertical path from the initial orbitals to the current orbitals, $\mathbf{C}_1'$. However, one may first apply the horizontal transform $\mathbf{H}$ to $\mathbf{C}_0$ to obtain a new set of initial orbitals, $\mathbf{C}_0'$, such that the initial energy is unaffected. Then equation (28) allows us to determine a new vertical step $\tilde{\mathbf{V}}$ that connects these orbitals to the current set. By repeated application of this procedure, one can transform a sequence of alternating vertical and horizontal steps $\{\mathbf{V}_1, \mathbf{H}_1, \mathbf{V}_2, \mathbf{H}_2, \mathbf{V}_3, \mathbf{H}_3, \ldots\}$ to obtain

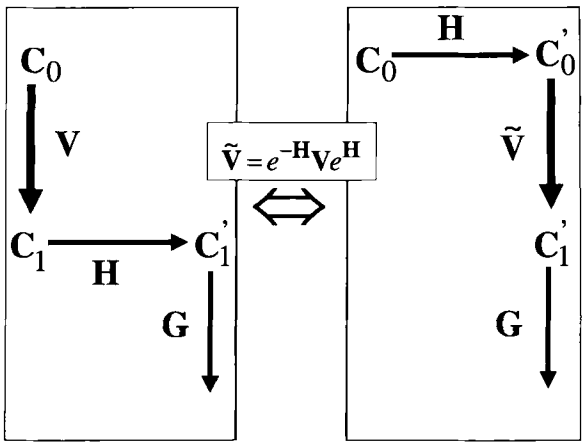

Figure 1. Vertical step followed by a horizontal step can be rewritten as the horizontal step followed by a transformed vertical step.

a trajectory containing only vertical steps $\{\tilde{\mathbf{V}}_1, \tilde{\mathbf{V}}_2, \tilde{\mathbf{V}}_3, \ldots\}$ that arrives at the same final set of orbitals provided that the set of initial orbitals is transformed by the sequence of horizontal transformations $\{\mathbf{H}_1, \mathbf{H}_2, \mathbf{H}_3, \ldots\}$. From a geometric point of view, this trajectory of vertical steps has taken the 'straightest' path to the current point while still remaining on the surface. Since the straightest path also has the least curvature, convergence acceleration should be most efficient along this path.

In summary, our algorithm for SCF orbital optimization looks like this:

(1) Obtain an initial set of (orthogonal) orbital coefficients $\mathbf{C}_0$.
(2) Pseudo-canonicalize the orbitals. Save the transformation matrix.
(3) Transport the gradients $\{\mathbf{G}_i\}$ and steps, $\{\mathbf{S}_i\}$ from previous iterations to the current set of pseudo-canonical orbitals using equation (28).
(4) Compute the gradient, $\mathbf{G}_{i+1} = \mathrm{d}E/\mathrm{d}\mathbf{V}$. It is easily verified that $\mathbf{G}_{\mathrm{ov}} = \mathbf{F}_{\mathrm{ov}}$, where $\mathbf{F}$ is the pseudo-canonical Fock matrix.
(5) Convert the gradients and steps into energy weighted coordinates

$$G_{ia} \rightarrow \frac{G_{ia}}{B_{ia,ia}^{1/2}} \quad \text{and} \quad S_{ia} \rightarrow S_{ia}B_{ia,ia}^{1/2}, \tag{29}$$

where $\mathbf{B}$ is the diagonal Hessian (equation (23)).
(6) Build the BFGS Hessian (equation (20)) and use it to compute the approximate Newton–Raphson step (equation (18)).
(7) Convert the BFGS step $\mathbf{S}_{i+1}$ into a rotation,

$$S_{ia} \rightarrow \frac{S_{ia}}{B^{1/2}_{ia,ia}}. \quad (30)$$

(8) Update the orbitals using

$$\mathbf{C}_{i+1} = \mathbf{C}_i e^{\mathbf{S}}_{i+1}. \quad (31)$$

(9) If convergence has not been achieved, return to step 2.

We have found that this algorithm is extremely robust. The only weakness is that, since BFGS gives only an approximate step, there is the possibility that the energy will go up on a given iteration. If this happens, it is useful to perform an approximate line search along the previous step, making use of the information at the current and previous points. This takes care of the possibility that the BFGS step was in the right direction but just too long. If even this fails to lower the energy, it almost always indicates that the step, and therefore the BFGS matrix, is bad. Thus, if the line search fails, it is best to re-set the BFGS space, back up to the best previous point and simply take a steepest descent step.

Steps 1–9 together with the failsafe option of a line search define the geometric direct minimization (GDM) algorithm for the solution of the SCF equations. It should be mentioned that most of what has been developed here presumes there is one set of orbitals that is desired, as in an RHF calculation. In the case of spin unrestricted orbitals, this is generalized trivially by simply applying rotations to the alpha and beta orbitals separately. The restricted open shell case is more complicated and has not been implemented, although in principle there is no obstacle to such an approach.

3. Results

The GDM algorithm has been implemented in Version 2.0 of the 'Q-Chem' software package [24]. For comparison, we compare the rate and reliability of convergence for the current algorithm with the results of Pulay's DIIS procedure [1, 2]. All closed shell molecules used spin-restricted orbitals and all open shell species were unrestricted. The iterations were deemed converged if the energy change fell below 1×10^{-10} E_h and the RMS gradient fell below 1×10^{-7} in less than 256 iterations. For the purposes of discussion we shall refer to the lowest energy obtained by any of the algorithms as the 'global minimum', although we cannot exclude the possibility that there might be a solution still lower in energy that none of these approaches can find. Finally, to present an equal comparison, the cases where DIIS fails to converge have been removed from the statistical analysis and will be discussed separately.

3.1. *The G2 set*

We have performed SCF calculations for the 56 molecules whose dissociation energies were utilized in the calibration of the G2 method [25]. The set contains a variety of main group compounds which should provide an unbiased picture of the performance of the different convergence acceleration techniques. We chose the 6-311++g** basis [26, 27] and the generalized Wolfsberg–Helmholtz (GWH) guess [28] for all calculations and have considered both the Hartree–Fock and the B3LYP [29] methods.

A statistical summary of the results obtained for these molecules is contained in table 1, from which it can be seen that generally DIIS converges quite rapidly for these systems, but fails to find a solution in two cases (B3LYP for the OH and CH radicals). GDM is quite competitive with the standard theory, taking on average only about 3 iterations longer to achieve convergence, and is successful in converging the case where DIIS fails. Hence, for these main group systems GDM improves the robustness of DIIS without significantly increasing the cost.

GDM demonstrates a tendency to find local minima, whereas DIIS seems to find the global minimum more consistently. The reason for this is clear; in the formulation of the current method we have rigorously enforced the orthogonality constraint (4), and thus the search takes place only in the space of possible solutions. On the other hand, the DIIS extrapolated Fock matrix may not be derivable from a set of orthonormal orbitals; orthonormality is enforced because the new orbitals are chosen as the eigenvectors of the extrapolated Fock matrix. Thus, DIIS can temporarily leave the surface of constraint in order to obtain the new extrapolated orbitals. In cases where the surface is bumpy, this allows one to 'tunnel through' barriers rather than having to climb over them. Clearly this increases the ability of DIIS to escape from regions near a local minimum, and explains the observed tendency to arrive at lower energy solutions.

Table 1. Convergence statistics for the 56 molecules in the G2 test set [25].

Method	Average iterations	Maximum iterations	Local minima	Did not converge
DIIS/HF	13.4	26	0	0
DIIS/B3LYP	11.8	17	0	2
GDM/HF	16.3	42	5	0
GDM/B3LYP	16.3	58	5	0
DIIS-GDM/HF	13.8	24	0	0
DIIS-GDM/B3LYP	13.9	24	0	0

The propensity of GDM to find local minima is beneficial in many cases. It often happens that the lowest energy solution for a correlated calculation such as MP2 or CCSD is not the same as for the HF solution. In these cases, it is highly desirable to have a method that can be induced to land consistently on this solution. Similarly, when one considers energies collected at several different geometries, as might occur in a geometry optimization or during a molecular dynamics simulation, it is usually understood that one wishes to consider the same state at all geometries, regardless of whether it is the global minimum for the current structure. In both these cases, GDM would seem to be the preferable alternative.

Sometimes, of course, convergence to the global minimum is exactly what is desired. In these cases, a robust approach can be formulated by performing DIIS extrapolation until the RMS Gradient is below, say 0.01. In this scheme, effectively DIIS acts as to pre-converge the orbitals that are input into the GDM procedure. We present the results for this approach under the heading DIIS-GDM in table 1, and it is seen that the hybrid approach retains the rapid convergence of both DIIS and GDM for these cases, combining the robustness of the GDM algorithm with the ability of DIIS to find the lowest energy solution.

3.2. *Transition metal complexes*

Transition metal systems present an interesting challenge for SCF convergence, since often there are extremely large numbers of low energy critical points that an algorithm must sort through in order to arrive at a suitable minimum. This makes it almost impossible for a convergence algorithm to consistently pick out the global minimum from among the swarm of candidates. This can be aided by tailoring the initial guess to treat a battery of organometallic systems well [30], and so our task for these cases is focused on discovering an algorithm that converges quickly and consistently to a minimum, with the presumption that the convergence can be shunted towards the global minimum by suitable adjustment of the initial guess.

To see how well GDM deals with the abundance of critical points and near-degeneracies in these cases, we have run calculations on the first-row transition metal carbonyl (MCO^+) and dicarbonyl ($M(CO)_2^+$) cations of [31] and the first-row transition metal–methylene cations (MCH_2^+) of [32]. Our calculations employed the 6-31g* basis [33] and the GWH guess [29]. Since we make no attempt here to include relativistic corrections, we use the non-relativistic optimized geometries [31, 32].

A statistical summary of the convergence rates is presented in table 2, showing that GDM is significantly slower than DIIS for these cases, although it still succeeds in converging in all cases where DIIS fails. The convergence of GDM is slowed for these molecules due to the presence of saddle points. With GDM, often one observes a rapid decrease in step size as a saddle point is approached, which means it takes very many small steps to traverse a saddle point and continue with the minimization. It is not completely clear why DIIS has no such difficulty; in some cases the problem is moot because DIIS simply converges to the saddle point, which clearly is undesirable, but in other cases, DIIS seems to avoid these problem areas.

Table 2. Convergence statistics for the 27 first row transition metal complexes MCO^+, $M(CO)_2^+$ and MCH_2^+

Method	Average iterations	Maximum iterations	Local minima	Did not converge
DIIS/HF	33.1	101	8	4
DIIS/B3LYP	26.1	58	9	2
GDM/HF	88.6	216	13	1
GDM/B3LYP	77.5	170	7	0
DIIS-GDM/HF	30.8	56	3	0
DIIS-GDM/B3LYP	31.8	104	3	0

For transition metal complexes, the robust convergence of GDM can be combined with DIIS's ability to deal with saddle points using the hybrid DIIS-GDM approach. As can be seen in table 2, DIIS-GDM converges at essentially the same rate as DIIS, and the robustness of GDM is completely retained. Further, it is interesting to note that DIIS-GDM tends, on average, to converge to even lower energy solutions than either DIIS or GDM individually. This would seem to result from the fact that running a few DIIS iterations effectively supplies GDM with an improved initial guess that lies within the basin of attraction of a different (and more reliable) minimum.

3.3. *Difficult cases*

It is instructive to present in detail those cases where DIIS fails to converge. The results of GDM and DIIS-GDM optimization for these systems are listed in table 3. These systems show the same general features that have been observed previously. GDM converges rapidly, except for one case (B3LYP for $ScCO^+$) where the procedure encounters a saddle point between the initial guess and the final result. Running DIIS for the first several iterations pushes the energy below the offending saddle point and convergence is then much more rapid. In other cases, the rate of convergence of the hybrid procedure is comparable with GDM. These systems illustrate the tendency of DIIS-GDM to find lower energy solutions than GDM alone, as the hybrid approach finds a lower solution for five of the seven cases. It is important to recognize that many of these

Table 3. Converges information for molecules where DIIS failed to converge (energies in E_h).

	GDM		DIIS-GDM	
Molecule	Iterations	Energy	Iterations	Energy
CH/B3LYP	22	−38.4941	23	−38.4941
OH/B3LYP	27	−75.7624	22	−75.7624
$NiCH_2^+$/HF	54	−1545.2996	33	−1545.2996
$NiCH_2^+$/B3LYP	29	−1547.0374	33	−1547.0561
$CoCO^+$/HF	31	−1493.6052	52	−1493.6643
$NiCO^+$/HF	34	−1619.0480	49	−1619.0866
$ScCO^+$/B3LYP	101	−873.6381	61	−873.6831
$Fe(CO)_2^+$/HF	32	−1487.3737	58	−1487.4712

cases could also have been converged by using standard 'tricks of the trade' in conjunction with DIIS, for example, by employing a level shift or damping the DIIS iterations. However, we think the GDM approach is prefereable to these techniques because it presents a unified solution to these problems.

4. Discussion

We have presented no estimates of the cost of this approach relative to DIIS. GDM is designed for the intermediate size regime where the cost is dominated by Fock builds rather than matrix manipulations, and therefore such considerations are not relevant. This covers the vast majority of computations done today. For extremely large molecules, linear scaling methods are a necessity, and density matrix-based treatments are expected to be much more efficient due to the exponential decay of the density for non-conducting systems. Much of the present algorithm could be rephrased readily in terms of the effects of the unitary transformation on the one-particle density matrix rather than the orbitals. Then, the locality of the density matrix in the atomic orbital basis could be exploited to perform matrix multiplications in a linear scaling fashion [34]. The only obstacle to this approach is that the orbital Hessian (23) requires diagonalization of the oo and vv blocks of the Fock matrix, and there is no well defined prescription for diagonalizing sparse matrices in linear time. If an alternative approximate Hessian could be obtained that did not require pseudo-canonical orbitals, the current algorithm could be translated very readily into a linear scaling density matrix-based scheme, very similar in spirit to that of [34].

There is one significant alteration that would need to be made in order to apply this approach to ROHF optimization or to active space correlation methods like CASSCF [19]. In both of these cases, instead of having two invariant subspaces (occupied and virtual) one has multiple invariant subspaces. In the case of ROHF, one has doubly occupied, singly occupied and unoccupied subspaces that are invariant to rotations within themselves. In the case of CASSCF [19], one has inactive occupied (o), inactive virtual (v) and active (a) subspaces. Considering the CASSCF case, the logical generalization of updating the orbitals by sequential ov rotations,

$$\mathbf{C}_{\text{new}} = \mathbf{C}e^{A_{\text{ov}}}, \tag{32}$$

is to perform a sequence of three rotations at each step

$$\mathbf{C}_{\text{new}} = \mathbf{C}e^{A_{\text{ov}}}e^{A_{\text{oa}}}e^{A_{\text{av}}}, \tag{33}$$

where the order of the rotations is arbitrary but should be the same at each iteration. Each of these three rotation classes could then be extrapolated sequentially using manipulations that are completely analogous to those presented here. For example, after the ov rotation has been performed, the vectors from previous iterations could be translated to the new coordinate frame using

$$\tilde{\mathbf{V}} = e^{A_{\text{ov}}^{\dagger}}\mathbf{V}e^{A_{\text{ov}}}. \tag{34}$$

The BFGS and approximate orbital Hessians could then be applied in exactly the same way, as has been done in [9]. The ability to perform an efficient search without having to resort to explicit calculation of the Hessian is extremely important for optimized orbital coupled cluster methods [18, 7, 6] where, as for SCF, the formation and inversion of the full Hessian is expensive.

5. Conclusions

In this work we have used basic principles of differential geometry to formulate a new approach to energy minimization for methods that depend on a set of orthonormal orbitals. The resulting approach, GDM, is competitive with DIIS for many systems and capable of converging many 'problem cases' where DIIS fails to find a solution. It is satisfying that this can be achieved by a rigorous geometric argument that does not resort to heuristic damping factors or level shifts.

For systems where DIIS converges, GDM shows a mild tendency to converge to higher energy solutions than DIIS. This happens primarily when the initial guess is far from the global minimum, and it is argued that this is a desirable characteristic in many situations. However, in case the GDM solution is not acceptable, we also present a hybrid DIIS-GDM approach that regularly gives energies that are as low as the DIIS solution but that retains the robustness of GDM. The hybrid procedure also tends to accelerate convergence significantly in cases where GDM is slow to converge.

It is clear that the source of the robustness of these procedures is the adherence to the direct minimization

strategy, which requires the energy to go down at every iteration. Whereas an extrapolation technique such as DIIS can oscillate between two fixed points, this is not allowed in a direct minimization, since one of the two points must be higher in energy and thus one half of the oscillation must involve an uphill step.

The GDM strategy has many potential applications due to the prevalence of the orbital optimization problem in electronic structure theory. One interesting direction involves the simultaneous updating of nuclear and electronic degrees of freedom [8, 23], which would have clear relevance for Car–Parrinello molecular dynamics [35], where the size of the timestep is determined mainly by the radius of reliable extrapolation of the Kohn–Sham orbitals along the trajectory. Since the current algorithm is simply the geometric generalization of a trajectory in the presence of an orthogonality constraint, it stands to reason that the success of this method for single-point problems could be extended readily to deal with molecular dynamics simulations.

Another interesting application of these principles would be to test similar approaches for active space correlation models [6, 19] that involve only a minor extension of the formulae presented here. Previous work [9] suggests that this avenue should be fruitful.

This research was supported by a grant from the National Science Foundation (CHE-9981997).

References

[1] Pulay, P., 1980, *Chem. Phys. Lett.*, **73**, 393.
[2] Pulay, P., 1982, *J. Comput. Chem.*, **3**, 556.
[3] Hamilton, T. P., and Pulay, P., 1986, *J. chem. Phys.*, **84**, 5728.
[4] Van Lenthe, J. H., Verveek, J., and Pulay, P., 1991, *Molec. Phys.*, **73**, 1159.
[5] Muller, R. P., *et al.*, 1994, *J. chem. Phys.*, **100**, 1226.
[6] Krylov, A. I., Sherrill, C. D., Byrd, E. F. C., Head-Gordon, M., 1998, *J. chem. Phys.*, **109**, 10669.
[7] Sherrill, C. D., Krylov, A. I., Byrd, E. F. C., Head-Gordon, M., 1998, *J. chem. Phys.*, **109**, 4171.
[8] Head-Gordon, M., and Pople, J. A., 1988, *J. phys. Chem.*, **92**, 3063.
[9] Chaban, G., Schmidt, M. W., and Gordon, M. S., 1997, *Theoret. Chim. Acta*, **97**, 88.
[10] Chancès, E., and Le Bris, C., 2000, *Intl. J. Quantum Chem.*, **79**, 82.
[11] Bacskay, G. B., 1981, *Chem. Phys.*, **61**, 385.
[12] Bacskay, G. B., 1982, *Chem. Phys.*, **65**, 383.
[13] Sano, T., and I'Haya, Y. J., 1991, *J. chem. Phys.*, **95**, 6607.
[14] Edelman, A., Arias, T. A., and Smith, S., 1998, *SIAM J. Matrix Anal. Applic.*, **20**, 303.
[15] Roothaan, C. C. J., 1951, *Rev. Mod. Phys.*, **23**, 69.
[16] Bobrowicz, F. B., and Goddard, W. A., 1977, *Methods of Electronic Structure Theory*, Vol. 3, edited by H. F. Schaefer III (New York: Plenum Press).
[17] Krieger, J. B., Li, Y., and Iafrate, G. J., 1992, *Phys. Rev.* A, **46**, 5453.
[18] Scuseria, G. E., and Schaefer, H. F., 1987, *Chem. Phys. Lett.*, **142**, 354.
[19] Roos, B. O., Taylor, P. R., and Siegbahn, P. E. M., 1980, *Chem. Phys.*, **48**, 157.
[20] Do Carmo, M. P., 1976, *Differential Geometry of Curves and Surfaces* (Prentice-Hall).
[21] Hutter, J., Parrinello, M., and Vogel, S., 1994, *J. chem. Phys.*, **101**, 3862.
[22] The BFGS method is discussed, e.g. in the popular *Numerical Recipes* books available at www.nr.com.
[23] Fischer, T. H., and Amlöf, J., 1992, *J. phys. Chem.*, **96**, 9768.
[24] Kong, J., White, C. A., Krylov, A. I., Sherrill, C. D., Adamson, R. D., Furlani, T. R., Lee, M. S., Lee, A. M., Gwatlney, S. R., Adams, T. R., Daschel, H., Zhang, W., Korambath, P. P., Ochsenfeld, C., Gilben, A. T. B., Kedziora, G. S., Maurice, D. R., Nair, N., Shao, Y., Besley, N. A., Maslen, P. E., Dombroski, J. P., Baker, J., Byrd, E. F. C., Van Voorhis, T., Oumi, M., Hirata, S., Hsu, C.-P., Ishikawa, N., Florian, J., Warshel, A., Johnson, B. G., Gill, P. M. W., Head-Gordon, M., and Pople, J. A., 2000, Q-Chem 2.0: A high performance ab initio electronic structure program package; *J. comput. Chem.*, **21**, 1532.
[25] Curtiss, L. A., *et al.*, 1991, *J. chem. Phys.*, **94**, 7221.
[26] Krishnan, R., Binkley, J. S., Seeger, R., and Pople, J. A., 1980, *J. chem. Phys.*, **72**, 650.
[27] Clark, T., Chandrasekhar, J., and Schleyer, P. v. R., 1983, *J. Comput. Chem.*, **4**, 294.
[28] Dupuis, M., and King, H. F., 1977, *Intl. J. Quantum Chem.*, **11**, 613.
[29] Becke, A. D., 1993, *J. chem. Phys.*, **98**, 5648.
[30] Vacek, G., Perry, J. K., and Langlois, J.-M., 1999, *Chem. Phys. Lett.*, **310**, 189.
[31] Barnes. L. A., Rosi, M., and Bauslicher, Jr., C. W., 1990, *J. chem. Phys.*, **93**, 609.
[32] Bauslicher, Jr., C. W., *et al.*, 1992, *J. phys. Chem.*, **96**, 6969.
[33] Hariharan, P. C., and Pople, J. A., 1973, *Theoret. Chim. Acta*, **28**, 213.
[34] Helgaker, T., Larsen, H., Olsen, J., and Jørgensen, P., 2000, *Chem. Phys. Lett.*, **327**, 397.
[35] Car, R., and Parrinello, M., 1985, *Phys. Rev. Lett.*, **55**, 2471.